Random packing of binary hard discs

2004 J. Phys.: Condens. Matter 16 6651

(http://iopscience.iop.org/0953-8984/16/37/002)

INSTITUTE OF PHYSICS PUBLISHING JOURNAL OF PHYSICS: CONDENSED MATTER

J. Phys.: Condens. Matter **16** (2004) 6651–6659 PII: S0953-8984(04)74699-8

Random packing of binary hard discs

Tsuyoshi Okubo and Takashi Odagaki

Department of Physics, Kyushu University, Fukuoka 812-8581, Japan

E-mail: t.okubo@cmt.phys.kyushu-u.ac.jp

Received 13 January 2004, in final form 13 January 2004
Published 3 September 2004
Online at stacks.iop.org/JPhysCM/16/6651
doi:10.1088/0953-8984/16/37/002

Abstract

Random dense packing of binary hard discs generated under the infinitesimal gravity protocol is investigated by a Monte Carlo simulation in the entire region of the size ratio and the concentration. When the size difference of the two species is small, the packing fraction of disc assembly becomes lower than that of the monodisperse system. Defining the adjacent neighbours of a disc through the radical tessellation, we show that the packing fraction can be related to the distance of adjacent discs and that the suppressed packing fraction is caused by an increase of the adjacent neighbours which are not seen in the monodisperse system.

1. Introduction

Random packings of spheres serve as useful models for a variety of condensed matter systems. For example, the structure of amorphous metals, colloidal suspensions and deposition of particles are well described by random dense packing of spheres. Although the random packing of spheres has been studied for a long time for this reason, there are many unsolved problems for random packing.

Considering the fact that the packing fraction depends on the randomness of the system, Torquato *et al* have proposed a new concept of maximally random jammed state (MRJ) [1]. The MRJ state is defined as the structure that minimizes an order parameter among all jammed structures. It is mathematically well defined, and some order parameters were proposed to estimate for the density of the MRJ state. Although they determine several possible MRJ states, the order parameter which by itself can measure various types of order has not been found [1–3].

In the theoretical analysis of random dense packing, monodisperse spheres have well been investigated. In physical systems of interest, however, packing particles are often polydisperse, and it is not clear how polydispersity affects the random dense packing. Although random packing of binary hard discs has been studied as a function of size ratio and concentration [4–7], the effect of mixing on the packing has not been elucidated, and more elaborate analysis is necessary for practical applications.

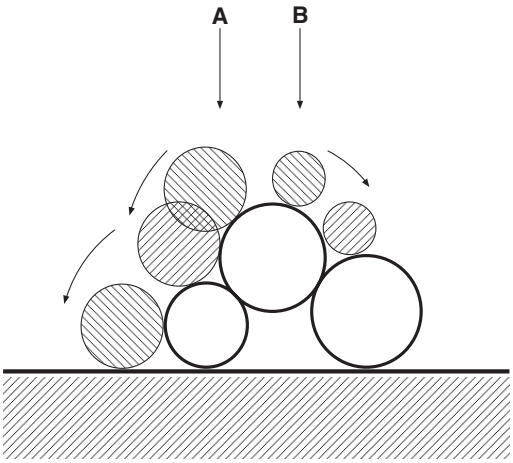

Figure 1. Schematic illustration of the infinitesimal gravity protocol used in this work. After contacting with another disc, each disc, A and B, rolls down around the target disc maintaining contact until it makes contact with another disc. If the horizontal coordinate of the centre of the rotated disc lies between centres of the other two discs, it cannot roll down further and settles there (B), or it rolls down around the new disc (A).

In this paper, we investigate the structure of a random dense packing of binary hard discs. It is known that the structure of packing depends on the protocol utilized to produce the packing. In order to avoid the subtlety in the definition of the MRJ due to the protocol dependence, we study the dense packing produced by the drop-and-roll or the infinitesimal gravity protocol using a Monte Carlo simulation. Although it is important to consider the MRJ state and jammed structure, it is worth studying the structure produced by this sequential protocol since in practical applications the packing structure of particles is produced by a fixed procedure such as molecular vapour deposition. It is supposed that the packing fraction of a random assembly of monodisperse discs is $\phi_{(2d)} \simeq 0.82$ [8, 9]. We obtain the dependence of the packing fraction on the ratio of the radius of the discs and the concentration. We also present an analysis of disc assembly using radical tessellation, which is a generalization of Voronoï tessellation. It is shown that the packing fraction is closely related to the distribution of distance between adjacent neighbours defined by radical tessellation. We describe the method for generating disc assemblies and show the results of simulation in section 2. In section 3, we propose a formalism to estimate the packing fraction using radical tessellation. In section 4, comparing our formalism with the results of numerical simulation, we give a discussion on the results. Our conclusion is given in section 5.

2. Simulation

2.1. Simulation method

We prepare a container of $L \times L$ with a periodic boundary condition in the horizontal direction. We introduce a disc above the container at a horizontal position selected randomly. The radius of the disc, which is R_S (small) or R_L (large), is chosen randomly at a given concentration x. In the infinitesimal gravity protocol, the disc is dropped vertically towards the bottom of the container. If the disc makes contact with a disc (the target disc) introduced earlier, it stops falling and rolls down around the target disc keeping contact (see figure 1). The rotation is continued until either its centre is as high as the centre of the target disc or it touches another

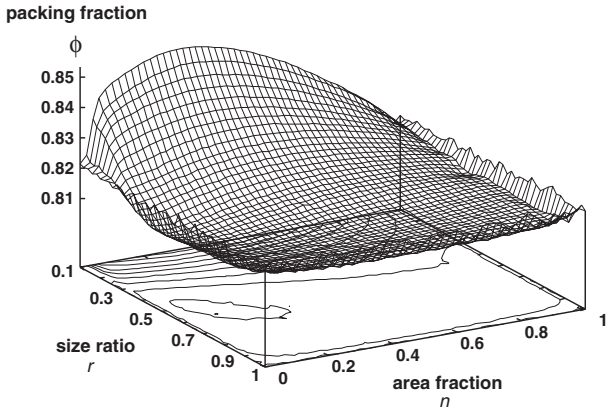

Figure 2. A 3D plot of the packing fraction of a binary hard disc assembly as a function of size ratio r and area fraction n. Each value was determined from an average of 20 samples. The contours are drawn from 0.81 to 0.85 every 0.05.

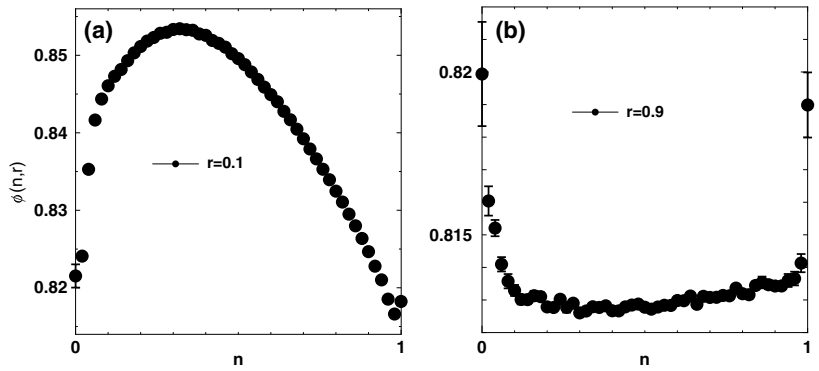

Figure 3. The packing fraction $\phi(n, r)$ of fixed r; (a) $r = 0.1$ and (b) $r = 0.9$. Each of the error bars indicates the root-mean-square error.

disc. In the former case, the disc starts falling again. In the latter case, the disc behaves in two different ways depending on the arrangement of the three discs. If the horizontal coordinate of the centre of the rotated disc lies between centres of the other two discs, it cannot roll down further and settles there (B in figure 1). If not, it rolls down around the new disc (A in figure 1). When the disc settles into a stable position or makes contact with the base line, it is fixed there. We repeat the process until the container is filled with discs.

In our Monte Carlo simulation the system size is set to $L/2R_{\mathrm{L}} = 100$ and discs at given fraction x of the smaller disc are packed up to a height of $140 \times 2R_{\mathrm{L}}$. To reduce the effects of the boundaries, upper and lower $20 \times 2R_{\mathrm{L}}$ layers are discarded (so that the remaining area is $100 \times 100 \times 4R_{\mathrm{L}}^2$), and then the packing fraction ϕ is calculated as a function of the disc size ratio $r = R_{\mathrm{S}}/R_{\mathrm{L}}$ and the area fraction of smaller discs $n = xR_{\mathrm{S}}^2/\{(1-x)R_{\mathrm{L}}^2 + xR_{\mathrm{S}}^2\}$.

2.2. Results

The packing fractions $\phi(n, r)$ obtained from the Monte Carlo simulation are illustrated in figure 2. Note that $\phi(0, r) = \phi(1, r) = \phi(n, 1) = \phi(n, 0) = \phi_{(2\mathrm{d})} \simeq 0.82$. For $r \simeq 0$, as n

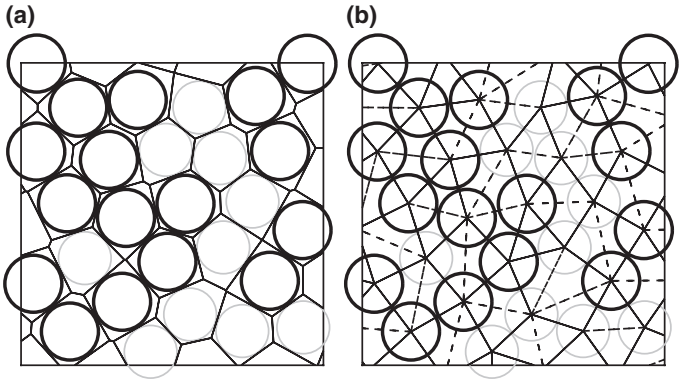

Figure 4. Example of radical tessellation, (a), and generalized Delaunay triangles, (b), of an assembly of binary discs, where difference of size is indicated by black and grey circles. In (b), the solid lines connect the adjacent neighbours which contact each other and the dashed lines represent the bonds which connect the separate adjacent neighbours.

is increased from $n = 0$, $\phi(n, r)$ increases dramatically, as shown in figure 3(a); as Odagaki and Hoshiko [7] described, this feature can be understood as the result of the vacant spaces between larger discs being filled by smaller discs. The increase of packing fraction reaches a maximum at a certain n where the vacant spaces are almost filled up, and decreases to the value for the monodisperse assembly. On the other hand, $\phi(n, r)$ for $r \simeq 1$ shown in figure 3(b) decreases from $\phi_{(2d)}$ as n is increased from $n = 0$, and is almost constant over the wide range of n until it increases to $\phi_{(2d)}$ near $n = 1$. The decrease of $\phi(n, r)$ is due to the fact that the smaller disc, which is too large to fill the vacant spaces, replaces the larger discs and destroys the structure formed by larger discs.

In the intermediate region of r, $\phi(n, r)$ behaves like a mixture of the two extreme behaviours. As r increases from $r = 0$, the peak of $\phi(n, r)$ shifts to larger n and decreases in magnitude, and the minimum of $\phi(n, r)$ appears at smaller n. Because the decrease of $\phi(n, r)$ near $n = 0$ is the result of the replacing effect described above, the difference between the minimum value and $\phi(0, r)$ increases as the disc size ratio reaches $r = 1$.

3. Radical tessellation analysis

The radical tessellation introduced by Gellatly and Finney [10] is a generalization of Voronoï tessellation defined for monodisperse spheres to polydisperse spheres, which was first used extensively by Troadec *et al* [11] for dilute assemblies of binary discs.

In the Voronoï tessellation in two dimensions, the space is partitioned into a set of polyhedra where each edge is drawn as the perpendicularly bisecting line between two discs. The radical tessellation is constructed as follows. First, we draw a line produced as the locus of points from which the lengths of the tangents to two discs are equal. Secondly, we draw these lines for all pairs of discs and we assign a tessellation to a disc. When the radical tessellation is performed, each disc is surrounded by a convex polyhedron which fills the space without gaps. This property is the same as the Voronoï tessellation. At a vertex of these polyhedra, only three lines meet at a time in the random assemblies. We define the two discs as adjacent neighbours when radical cells of the two discs have one edge in common, and connect centres of all adjacent neighbour pairs to form a triangular network (see figure 4).

It should be mentioned that this construction of a triangular network is different from one introduced by Dodds *et al* [12]. The construction by Dodds *et al* is based on the

Voronoï tessellation for the centres, and the surface of Voronoï polyhedra may cut the particles. Our method based on the radical tessellation is known to be better for polydisperse systems [10].

For an infinite system, the mean number of adjacent neighbours for each disc Z_m is equal to 6, which is a consequence of Euler's condition, and therefore the number of triangles included in the system is twice as many as the number of discs. As a result, the packing fraction of the system ϕ is expressed in term of the mean area of triangles A_m,

$$\phi = \frac{\pi \langle R^2 \rangle}{2A_m} \tag{1}$$

where $\langle R^2 \rangle$ is the mean squared radius of discs in the system; for the binary disc under consideration, $\langle R^2 \rangle = (1-x)R_L^2 + xR_S^2$.

In the binary disc assembly, the triangles can be classified into four types according to the sizes of the three discs at the vertices of a triangle: (LLL), (LLS), (LSS) and (SSS). In terms of the mean area of the triangles A_{ijk} and the probability of finding them P_{ijk}, the mean area A_m is expressed as

$$A_m = P_{LLL}A_{LLL} + P_{LLS}A_{LLS} + P_{LSS}A_{LSS} + P_{SSS}A_{SSS}. \tag{2}$$

The probability P_{ijk} can be expressed in terms of the probability P_i which represents the probability of finding an i-type disc at a vertex of a triangle as

$$P_{LLL} = P_L^3, \qquad P_{LLS} = 3P_L^2P_S, \qquad P_{LSS} = 3P_LP_S^2, \qquad P_{SSS} = P_S^3. \tag{3}$$

If the assembly of discs is random, P_i is in proportion to the fraction, x_i, of i-type discs, and the mean number of adjacent neighbours of an i-type disc, Z_i (Dodds model [12]):

$$P_i = x_i \frac{Z_i}{Z_m} \tag{4}$$

where Z_m is the mean number of adjacent neighbours around a disc and $Z_m = x_LZ_L + x_SZ_S$.

The mean area A_{ijk} can be roughly estimated from the mean length of the bonds. There are three types of bonds, b_{ij}, according to the species of discs at each side of a bond. Considering the mean length of the bonds $\langle b_{ij} \rangle$ and the combination of them, we can form four different triangles. Instead of dealing with the mean area A_{ijk} directly, we approximate A_{ijk} by a_{ijk}, which is the area of these triangles. Using Helon's formula, a_{ijk} is expressed as

$$a_{ijk} = \sqrt{s(s - \langle b_{ij} \rangle)(s - \langle b_{jk} \rangle)(s - \langle b_{ki} \rangle)} \tag{5}$$

where

$$s = \tfrac{1}{2}(\langle b_{ij} \rangle + \langle b_{jk} \rangle + \langle b_{ki} \rangle). \tag{6}$$

Although this evaluation ignores the correlation of bonds which compose a triangle, as shown in next section, it is adequate to describe the behaviour of the packing fraction ϕ. Using equations (1)–(4) and the approximation $A_{ijk} \simeq a_{ijk}$, the packing fraction $\phi(n, r)$ can be calculated from Z_i and $\langle b_{ij} \rangle$ as

$$\phi \simeq \frac{\pi \langle R^2 \rangle}{2a_m} \tag{7}$$

where a_m is the approximate mean area defined by equation (2) with a_{ijk} in place of A_{ijk}.

4. Discussion

As we discussed in section 3, the packing fraction $\phi(n, r)$ can be calculated from the mean adjacent neighbour numbers Z_i and the mean bond lengths $\langle b_{ij} \rangle$ using equation (7). We apply

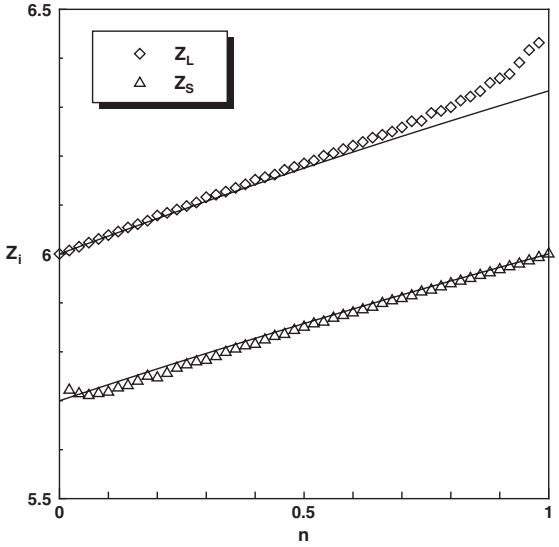

Figure 5. The mean number of adjacent neighbours around each species with $r = 0.9$ against n from simulation. The diamonds and triangles represent the mean number of adjacent neighbours around the larger disc and smaller discs respectively. The two solid lines denote equation (9).

this analysis to the case of $r \simeq 1$, where the packing fraction of binary discs becomes lower than that of monodisperse discs in our Monte Carlo simulation.

In figure 5, Z_i obtained from our simulation for $r = 0.9$ is shown. This form of Z_i is well explained by the following assumption. In a generalized Delaunay triangle geometry the minimum number of adjacent neighbours of a disc is 3 for each disc. Then we assume that $Z_i - 3$ is proportional to the length of circumference $2\pi R_i$; this leads to

$$\frac{Z_{\mathrm{L}} - 3}{Z_{\mathrm{S}} - 3} = \frac{R_{\mathrm{L}}}{R_{\mathrm{S}}}. \tag{8}$$

This, combined with the condition $Z_{\mathrm{m}} = 6$, leads to an approximate expression for Z_i,

$$Z_i = 3 + \frac{3R_i}{\langle R \rangle} \tag{9}$$

where $\langle R \rangle = (1-x)R_{\mathrm{L}} + xR_{\mathrm{S}}$ is the mean radius of discs in the system. This is also illustrated in figure 5. Equation (9) is in good agreement with the simulation for $r = 0.9$.

It is worth noting that for smaller r the deviation from equation (9) increases. This is due to increase of the vacant spaces where one more smaller disc can be put. In the assembly built up by infinitesimal gravity protocol at smaller r, these vacant spaces often exist around larger discs. It decreases the effective circumference length of the larger disc and hence the left-hand side of equation (8) becomes less than $R_{\mathrm{L}}/R_{\mathrm{S}}$.

The next step to calculate $\phi(n, r)$ using equation (7) is to estimate the mean length of each bond. In this stage, we use the information given by the simulation. As an example, we obtained $\langle b_{ij} \rangle$ as a function of n for $r = 0.9$ from the simulation and calculated $\phi(n, r = 0.9)$, which is illustrated in figure 6. $\phi(n, r)$ calculated from $\langle b_{ij} \rangle$ and Z_i is qualitatively in good agreement with the behaviour observed in the simulation. The quantitative difference between the simulation and our estimation mainly comes from the approximation that ignores correlations among the three sides constructing a generalized Delaunay triangle. We define the correction factor by $C_{\mathrm{cor}} \equiv \phi_{(2\mathrm{d})}/\phi(0, r) \simeq 1.043$ and show $\tilde{\phi}(n, r) = C_{\mathrm{cor}}\phi(n, r)$ in

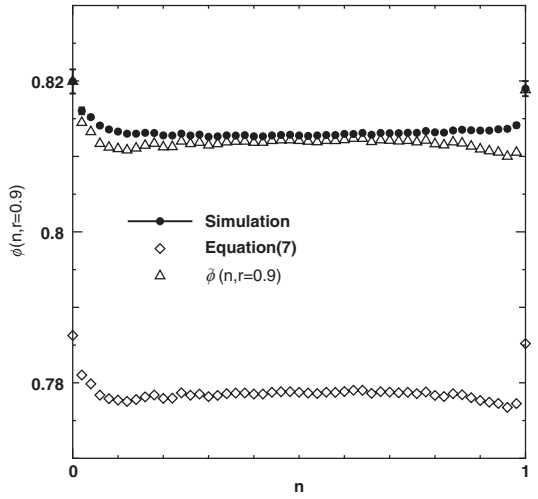

Figure 6. The packing fraction $\phi(n, r = 0.9)$ obtained from simulation (black circles) and equation (1) (diamonds). In equation (1), the mean area, $\langle A_{\mathrm{m}} \rangle$, was evaluated approximately from the mean bond lengths, $\langle b_{ij} \rangle$, in the simulation and the mean number of adjacent neighbours, Z_i, from equation (9). The modified packing fraction is also shown (triangles). It was multiplied by a constant so that the value at $n = 0$ agrees with the simulation.

figure 6. The very good agreement of $\tilde{\phi}(n, r)$ with the simulation indicates that if we know packing fraction of ideal discs, we can estimate the packing fraction from mean bond length at least for $r \simeq 1$.

It is worth mentioning that the correction factors arise from the correlation between the bond lengths which constitute a triangle. In our model, the mean area of the triangles is calculated assuming an uncorrelated bond length, but using the correction factor which involves information of bond length correlation in the monodisperse system, we can estimate the packing fraction of a binary disc assembly.

So far, the mean bond length has been obtained from the simulation. To estimate the packing fraction when n and r are given, we must know $\langle b_{ij} \rangle$ as a function of (n, r). To this end, we analyse the bond lengths in detail. The bond length distribution in our simulation is illustrated in figure 7. To compare with the equal disc assembly ($n = 0$ or 1) and the binary mixture assembly, we realize that the major difference of bond distributions is in the behaviour of the long length regime. In the equal disc assembly there is a discontinuity at a certain length, b_{ij}^c, over which the frequency is almost equal to zero. In the binary assembly, however, the frequency over b_{ij}^c has a non-zero value and decreases smoothly to zero. b_{ij}^c is in good agreement with the maximum value of the bond length when the contact disc network forms a quadrilateral, and it can be calculated from the definition of radical tessellation (see figure 4(b)). To evaluate the effects of this *tail*, we have defined the mean bond length from a fictitious bond length distribution in which the tail part is discarded. Figure 8 shows the packing fraction calculated from the fictitious bond length distribution. The packing fraction thus obtained behaves completely differently from the simulation; it is convex upwards at the centre. This indicates that, although the tail is small compared with the whole distribution, the behaviour of the tail greatly affects the packing fraction.

This fact complicates the estimation of the mean bond length because the tail comes from polygons which have more than four edges in the contact disc network and we have not so far estimated the mean bond length as a function of (n, r) with sufficient accuracy.

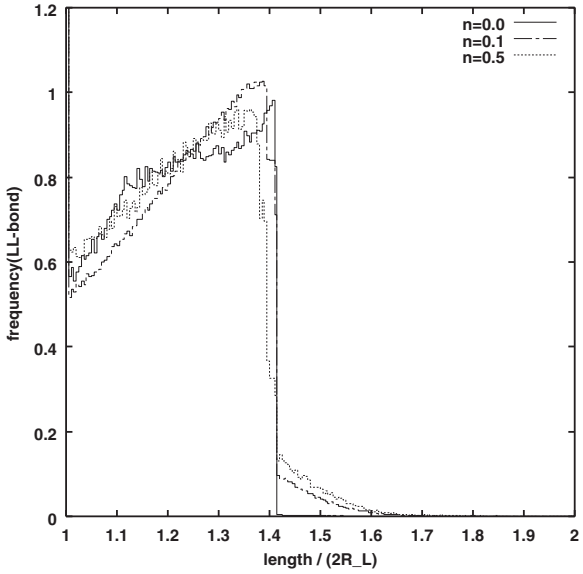

Figure 7. The distribution function of LL-bond length at $r = 0.9$. The solid, dash–dot and dot curves correspond to $n = 0.0$ (the equal disc assembly), $n = 0.1$ and $n = 0.5$. Note that each distribution function has a delta function-like peak at the length which equals $2R_{\mathrm{L}}$ because each disc must touch more than one disc in the assembly to be stable under gravity.

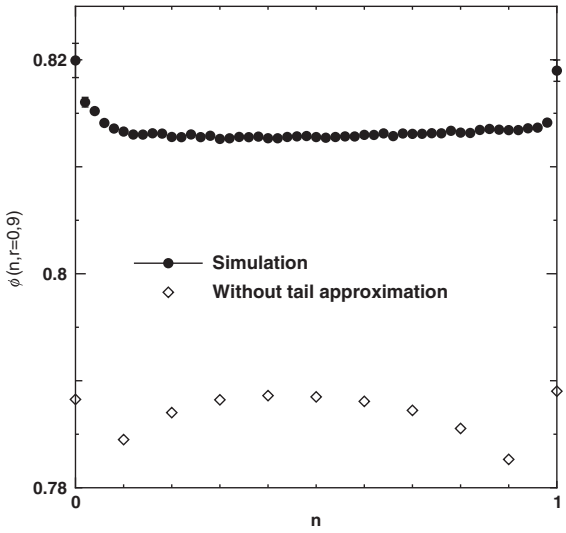

Figure 8. The packing fraction calculated from the tail-excepted bond length distribution function at $r = 0.9$ against n (diamonds). The solid circles are the packing fraction obtained from the simulation at the same r. The approximate packing fraction is very different, even qualitatively, from the simulation.

To obtain the form of $\phi(n, r)$ at $r \simeq 1$, we used equation (1) and paid attention to the mean area A_{m} instead of the packing fraction $\phi(n, r)$. If the disc assembly is sufficiently jammed, the areas of triangles are limited within a narrow range around the mean value, and

therefore the mean area, A_m, would be comparatively easily estimated. At smaller r, however, the assembly of binary discs has some large vacant spaces in the infinitesimal gravity protocol. As a result, the areas of the triangles are distributed in a wider range, so that estimating the mean area A_m is more complicated.

Recently it has been shown that the jamming category which the disc assembly belongs to plays an important role in determining the packing fraction [13]. For hard disc assemblies, three jamming categories have been introduced by Torquato *et al*: local, collective and strict [14]. By direct observation of the structure we conclude that the assemblies in our simulation belong to local jammed structure, at least when the size difference between two species is small. On the other hand, when the size difference is larger, we found that the larger discs are locally jammed but several smaller discs are not jammed. Although it is worth determining the precise jamming category of our assemblies, it is beyond the scope of this paper since we restrict our analysis to disc assemblies produced by a given protocol.

5. Conclusion

In this paper, we studied the random packing of binary hard discs produced by the drop-and-roll protocol. From Monte Carlo simulations, we obtained the packing fraction as a function of the disc size ratio r and the area fraction of smaller discs n. If r is sufficiently small, the packing fraction increases at first as n increases, due to the smaller discs filling in vacant spaces among the larger disc assembly, and then decreases to the packing fraction of the monodisperse system. On the other hand, if the size difference between two discs is small, the packing fraction decreases with increasing n at first, is almost constant over a wide range of intermediate values of n, and increases to the equal disc value near $n = 1$. We also applied the radical tessellation analysis to the binary disc assembly and showed that the behaviour of the packing fraction can be reproduced qualitatively from the mean bond length $\langle b_{ij} \rangle$ at least at $r \simeq 1$. We also concluded that the tail of the bond length distribution plays a significant role in determining the packing fraction. The tail arises from polygons which have more than four edges in the contact network, and makes estimation of packing fraction complicated.

Acknowledgment

This work was supported partially by the research fund from the Ministry of Education, Sports and Culture.

References

[1] Torquato S, Truskett T M and Debenedetti P G 2000 *Phys. Rev. Lett.* **84** 2064
[2] Truskett T M, Torquato S and Debenedetti P G 2000 *Phys. Rev.* E **62** 993
[3] Kansal A R, Torquato S and Stillinger F H 2002 *Phys. Rev.* E **66** 041109
[4] Visscher W M and Bolsterli M 1972 *Nature* **239** 504
[5] Bideau D, Gervois A, Oger A and Troadec J P 1986 *J. Physique* **47** 1697
[6] Barker G C and Grimson M J 1989 *J. Phys.: Condens. Matter* **1** 2779
[7] Odagaki T and Hoshiko A 2002 *J. Phys. Soc. Japan* **71** 2350
[8] Quickenden T I and Tan G K 1974 *J. Colloid Interface Sci.* **48** 382
[9] Berryman J G 1983 *Phys. Rev.* A **27** 1053
[10] Gellatly B J and Finney J L 1981 *J. Non-Cryst. Solids* **50** 313
[11] Troadec J P, Gervois A, Annic C and Lemaître J 1994 *J. Physique* I **4** 1121
[12] Dodds J A 1975 *Nature* **256** 187
[13] Donev A, Torquato S, Stillinger F H and Connelly R 2004 *J. Appl. Phys.* **95** 989
[14] Torquato S and Stillinger F H 2001 *J. Phys. Chem.* B **105** 11849